JAAS

Accepted Manuscript

This is an *Accepted Manuscript*, which has been through the Royal Society of Chemistry peer review process and has been accepted for publication.

Accepted Manuscripts are published online shortly after acceptance, before technical editing, formatting and proof reading. Using this free service, authors can make their results available to the community, in citable form, before we publish the edited article. We will replace this *Accepted Manuscript* with the edited and formatted *Advance Article* as soon as it is available.

You can find more information about *Accepted Manuscripts* in the Information for Authors.

ROYAL SOCIETY OF CHEMISTRY

www.rsc.org/jaas

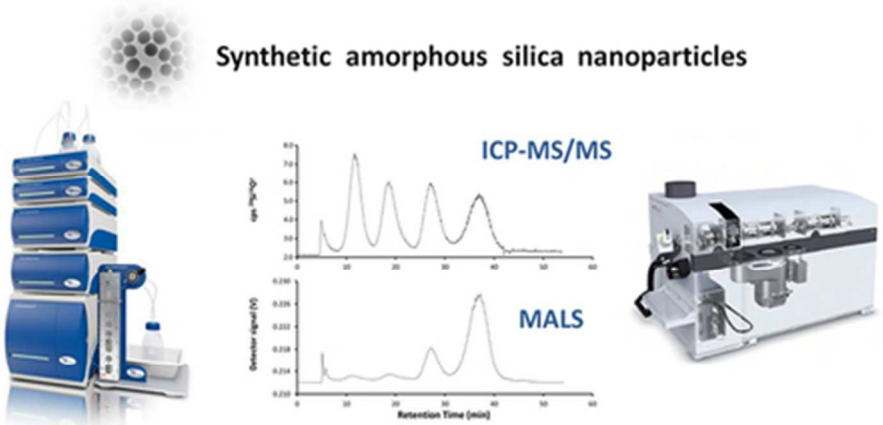

39x19mm (300 x 300 DPI)

Reliable and sensitive analytical method for the simultaneous determination of size and mass concentration of silica nanoparticles sized 20-200 nm

Quantitative characterization of silica nanoparticles by asymmetric flow field flow fractionation coupled with online multiangle light scattering and ICP-MS/MS detection

Federica Aureli, Marilena D'Amato, Andrea Raggi, Francesco Cubadda*

Department of Food Safety and Veterinary Public Health, Istituto Superiore di Sanità - Italian National Health Institute, Rome, Italy.

** Corresponding author*
Viale Regina Elena 299, 00161 Rome, Italy
e-mail: francesco.cubadda@iss.it
phone +39 06 49903643
fax +39 06 49902540

Abstract

Synthetic amorphous silica is one of the two commodity materials dominating the market of nanomaterials in terms of production volume, used in several industrial applications and found in a wide variety of consumers' products including medicines, toothpastes, cosmetics and food. Recent evidence emerged that despite a long history of use further investigation is needed to exclude long-term effects on human health for specific applications, such as food. It is therefore important to have easy, reliable and sensitive analytical methods for the determination of nano-sized silica available.

In this work a method for the simultaneous determination of particle size and mass concentration of synthetic amorphous silica nanoparticles by asymmetric flow field flow fractionation coupled with online multiangle light scattering and ICP-MS/MS detection is described. Accurate dimensional characterization of the particles separated by FFF was achieved by means of both ICP-MS/MS detection with size calibrants and standardless sizing by MALS. Element-specific detection by ICP-MS/MS using all the three silicon isotopes, pre-channel mass-calibration with silica nanoparticles and post-channel mass-calibration with elemental standards were used to provide quantitative data on the silicon present in the size fractions separated online by FFF. The FFF-MALS-ICP-MS/MS method developed enabled dimensional and mass determination of silica particles over the size range of approximately 20-200 nm with satisfactory recoveries of analyte material. The method was successfully applied to the characterization of two test samples, *i.e.* the reference material ERM-FD100 and a silica suspension having nominal diameters of 20 and 140 nm, respectively.

Introduction

According to the Second regulatory review on nanomaterials of the European Commission synthetic amorphous silica is one of the two commodity materials dominating the market of nanomaterials in terms of production volume (1.5 million tons in 2010).[1] Synthetic amorphous silica consists of nano-sized primary particles and may be found either as spherical SiO_2 nanoparticles in stabilised suspensions (colloidal silica or silica sols) or as particles with some degree of agglomeration or aggregation (precipitated silica, silica gels and fumed or pyrogenic silica). The various forms of synthetic amorphous silica are used in a wide variety of applications, including functional fillers in polymers, plastics, gel coats, silicone rubber applications, thermoplastic films, adhesives, electronics, paper industry, coatings, paints, inks, metal surface treatment, precision metal casting and refractory, photography, catalysis, textile, leather, building industry, reinforcement of elastomer products (primarily automotive tyres, footwear, rubber articles and cable sheathing), batteries and as drying agent (silica gels). Synthetic amorphous silica, including colloidal and surface-treated forms, is also widely used in topical and oral medicines, toothpastes, detergents and cosmetics. In the food and feed sector it is authorized as additive and used as anti-caking, antistatic and antifoaming agent, clarifying aid, carrier and as additive in food contact materials.[1-2] Silica nanoparticles also have great potential for a variety of diagnostic and therapeutic applications in medicine and for other applications.[2]

There is an increasing need for traceable methods enabling nanoparticle characterization as well as reference materials for quality assurance of measurements in the nano range.[3,4] They are required to support upcoming regulation,[5] enabling quality and compliance control of nano-products, and they are of crucial importance in assessing the still unsolved questions related to nano-safety. In the case of synthetic amorphous silica, a recent risk assessment concluded that there are concerns on long-term health effects due to the presence of this nanomaterial in food and further investigation on this topic is warranted.[6] In order to characterize the risks that nanomaterials may pose as a result of their

peculiar properties, both the understanding of their toxicological behaviour and the assessment of human exposure rely on availability of analytical methods capable to provide a thorough characterization of the nano-objects under investigation in testing media, biological samples, consumer's products (including food).[7]

Characterization of nanosilica particles dispersed in a liquid medium is usually performed by laser light-scattering techniques, mainly dynamic light-scattering (DLS).[8-10] Whereas these techniques perform well when dealing with samples of nanoparticles of a single size (monodispersed), they do not provide any information on chemical composition, have a low size resolution and are of limited use when samples containing particles of different sizes are analysed due to the inability to detect the presence of smaller particles among bigger ones. Hydrodynamic chromatography coupled to ICP-MS has also been used,[10] a technique that has the advantage of robustness but has poor size fractionation capabilities. Silica nanoparticles in aqueous suspensions has also been characterized by dynamic reaction cell ICP-MS in time resolved analysis (TRA) mode[11] but for the obtainment of conventional size distribution profiles single particle analysis would be required, which is currently limited by the poor size detection limits attainable for SiO_2[12] compared to the threshold of 100 nm of diameter generally accepted to define a nanomaterial as such[13]. Electron microscopy-based techniques (SEM/TEM) with energy-dispersive X-ray analysis (EDX) overcome all the above mentioned problems and are extremely accurate, but on the other hand they are costly, low-throughput and suffer from the need of extensive sample preparation for solvent removal that can potentially introduce bias in measuring the particle size distribution relative to the starting sample.[5, 14]

Owing to the widespread use in a variety of products up-to-date analytical methods for the characterization of nanosilica are needed, given the limitations of existing techniques and procedures. Field-flow fractionation (FFF) in combination with elemental and sizing detectors has emerged as a highly promising approach to separate and characterize nanoparticles,[15] but it has been

rarely applied to nanosilica. Sedimentation FFF combined with offline atomic absorption spectrometry for elemental analysis and SEM, TEM and DLS for size determination has been used for the characterisation of silica particles used as food additives.[16] On-line coupling of asymmetric flow FFF and ICP-MS has been achieved in a recent study of silica particles extracted from a coffee creamer matrix, but again an offline detector, *i.e.* TEM with EDX, was required as confirmatory sizing technique.[17]

In the present study, quantitative characterization of silica nanoparticles is accomplished by on-line coupling of asymmetric flow FFF with multiangle light scattering and ICP-MS/MS detection. Accurate dimensional characterization of the particles separated by FFF is achieved by means of both ICP-MS/MS detection with size calibrants and standardless sizing by multi angle light scattering (MALS). Element-specific detection by ICP-MS/MS, pre-channel mass-calibration with silica nanoparticles and post-channel mass-calibration with elemental standards are used to provide quantitative data on the recovery of the size fractions separated online by FFF. The use of ICP-MS/MS for the resolution of the polyatomic interferences affecting *m/z* 28-30 enabled for the first time to obtain fractograms based on all the three silicon isotopes.

Experimental

Instrumentation

The asymmetric flow FFF system used in this study consisted of a metal-free AF2000 MT model (Postnova Analytics, Landsberg am Lech, Germany), equipped with a flat separation channel (320 mm × 60 mm) of 280 mm length. A 350-µm spacer was used along with a 10 kDa molecular weight cut-off regenerated cellulose membrane (Lot. CF121212-1165513 Postnova Analytics) as accumulation wall. Manual injection was performed using a 20-µL loop. The carrier liquid consisted of a 0.1-µm filtered mixture containing 0.02% v/v of FL-70 - a commercially available alkaline surfactant mixture composed of water 88.8%, triethanolamine oleate 3.8%, sodium carbonate 2.7%, ethoxylated C12-14-secondary alcohols 1.8%, tetrasodium

ethylenediaminetetracetate 1.4%, polyethylene glycol 0.9%, sodium oleate 0.5%, sodium bicarbonate 0.1% (kindly donated by Dr. Catia Contado, University of Ferrara) - and NaCl 0.2 mM (suprapure grade, Merck KGaA, Darmstadt, Germany) at pH 8.5.

The fractionation system was coupled online to a PN3621 MALS detector (Postnova Analytics), with 21 observation angles, operated with linear polarized laser light at 532 nm (green) and a sampling time interval of 2 s per data point. Data from the MALS detector were processed using the Postnova AF2000 Control software (version 1.1.0.31). The spherical model was used for obtaining the radius of gyration on the basis of the angular dependence of scattered light recorded by the MALS detector.

ICP-MS detection was performed using an ICP-QQQ mass spectrometer (Agilent 8800, Agilent Technologies Inc., Tokyo, Japan). The instrument is equipped with an octopole-based collision/reaction cell (ORS^3 Cell) in-between the two quadrupole analyzers (Q1 and Q2) and was operated both in single quadrupole and MS/MS mode using either H_2 or O_2 (5.0 purity grade) as collision and reaction gases, respectively. The sample introduction system of the ICP mass spectrometer was replaced with inert (non-quartz) components, *i.e.* a platinum injector and a PFA concentric nebulizer with a double-pass PFA spray chamber cooled to 2 °C. The outlet of the MALS was connected to the inlet of the ICP nebulizer and the FFF eluate was mixed via a Teflon T-piece with a 0.1% nitric acid solution containing 2 µg/L Ge as internal standard by means of a peristaltic pump. Flow rates were checked on a daily basis by a flow-meter (SEDNA, E-POND, Vevey, Switzerland). The optimized operating parameters are summarized in Table 1.

Fig. 1 shows a scheme of the hyphenated FFF-MALS-ICP-MS/MS analytical platform used.

Materials and reagents

Near-monodisperse non-functionalized silica nanoparticle suspensions ('NanoXact') with nominal diameters of 20, 50, 80, 100, 120, 140, 160, and 180 nm were obtained by Nanocomposix (San

Diego, CA). They were supplied in Milli-Q water dispersions with pH 7.5-9.5 and had zeta-potentials in the range −29.8 mV to −52.2 mV.

For trueness assessment of particle size determination the reference material ERM-FD100 'colloidal silica in water' (IRMM, Geel, Belgium) was used. This material has a certified equivalent spherical diameter, expressed as number-based modal diameter obtained by electron microscopy, of 19.4 ± 1.3 nm. The intensity-weighted harmonic mean diameter (by DLS), the intensity-based modal Stokes diameter (by centrifuge liquid sedimentation) and the intensity-weighted mean diameter (by small angle X-ray scattering) have certified values of 19.0 ± 0.6 nm, 20.1 ± 1.3 nm, and 21.8 ± 0.7 nm, respectively. The suspension has a pH 9.7 and an indicative value for zeta-potential of −43 mV.

Ultrapure deionized water obtained by a Milli-Q Element System (Millipore, Molsheim, France) was used throughout. Calibrants and the internal standard (Ge) used for silicon measurements were obtained from certified solutions of 1 mg/mL (High Purity Standard, Charleston, SC) by dilution with acidified (HNO_3 67-69% v/v ultrapure grade, Carlo Erba Reagenti, Rodano, Italy) water as necessary. An internal quality control material (ISS-BL) prepared as detailed in Aureli et al.[12] was used for checking trueness of measurements. Ultrapure HNO_3, HF (47-51% v/v, Carlo Erba Reagenti, Rodano, Italy) and H_2O_2 (31% v/v, Merck KGaA, Darmstadt, Germany) were used for closed-vessel microwave digestion of this material and of the 20 and 50 nm particle suspensions as detailed elsewhere.[12]

Determination of total silicon by ICP-MS/MS

In the development of the ICP-MS/MS method, analytical calibration curves in 0.5% HNO_3 were built in the concentration range 1-100 ng/mL and parameters such as sensitivity (defined as the slope of the calibration curve), linearity, limit of detection (LoD, calculated as three times the standard deviation of the blank signal divided by the sensitivity factor), background equivalent concentration (BEC) and background signal were evaluated. The O_2 flow rate was optimized using

the FFF carrier solution as sample matrix and evaluating both the signal intensity and the BEC as a function of the cell gas flow rate.

All sample manipulations and analytical measurements were carried out in clean room conditions.

Determination of particle size and mass concentration of silica nanoparticles by FFF-MALS-ICP-MS/MS

The FFF method was developed to achieve controlled separation of particles over a size range of one order of magnitude (~20-200 nm as hydrodynamic diameter, d_h) with maximum recovery of analyte material. The silica nanoparticle suspensions with nominal diameters of 20, 50, 80, 100, 120, 160, 180 nm were characterized by FFF-MALS-ICP-MS/MS either in terms of size and mass fraction. Sizes were ascertained by converting the radius of gyration (r_g) obtained by MALS into d_h according to the relation r_g/r_h= 0.775 (d_h = $2r_h$) based on the consistent spherical shape of the particles used. The obtained results compared well with the d_h values reported on the manufacturer's certificate (Table 2), with an average absolute deviation in the range 1-4% except for the 20 nm sized particle that showed a value of 10%. As a result, the d_h values of the certificate were used as target values for calibration purposes. Particle size calibration was performed by injecting single monodisperse silica suspensions and plotting the known particle size against the resulting elution time. The curve-fitting equation was then determined.

Nominal particle mass concentration values provided by the manufacturer were in the range 9.9-10.7 mg/mL. Actual particle mass concentrations ascertained by ICP-MS/MS were found to be in the range 5.7-8.9 mg/mL and were used as target values for mass calibration. The total silicon content of the 20 and 50 nm sized particles was determined also after microwave digestion and an average absolute deviation of 2.4 % was obtained with respect to the undigested particles. The negligible difference observed between undigested particles and dissolved silica (after microwave digestion) suggested that ionic calibrants added post-FFF could be employed for the purpose of

quantifying silicon in the hyphenated analytical platform of the present study. Thus, a post-channel calibration approach[17] was adopted to quantify the silicon eluting from the FFF channel. To this end, increasing concentration of ionic Si (*i.e.* 0.5, 1, 2.5, 5, 10 µg/mL) were introduced into the eluent of the FFF-MALS system via a flow injection system with a 20-µL loop. Data were acquired in TRA mode and the integrated peak areas normalized to the internal standard were used to generate a calibration curve. Pre-channel mass calibration was used as well to account for possible losses occurring, e.g. in the FFF channel,[18] by performing injections of the 20, 50, 100, 180 nm nanoparticle dispersions at a concentration of 1.2, 2.5, 6, 12 µg/mL SiO_2. The loading points for both pre- and post-channel mass-size calibrations in the hyphenated analytical platform used are shown in Fig. 1.

The developed method was subjected to a detailed characterization in terms of analytical performance and applied to the size and mass determination of the reference material ERM-FD100 and of the silica suspension with 140 nm nominal diameter.

Results and discussion

Removal of interferences affecting Si detection by ICP-MS/MS

Sensitive and accurate silicon determination in standard, *i.e.* single quadrupole, mode is precluded owing to polyatomic interferences affecting the three naturally occurring isotopes ^{28}Si ($^{14}N^{14}N^+$, $^{12}C^{16}O^+$), ^{29}Si ($^{14}N^{15}N^+$, $^{14}N^{14}NH^+$, $^{13}C^{16}O^+$, $^{12}C^{16}OH^+$), and ^{30}Si ($^{15}N^{15}N^+$, $^{14}N^{15}NH^+$, $^{14}N^{16}O^+$, $^{13}C^{17}O^+$, $^{12}C^{17}OH^+$), whose natural abundances are 92.2%, 4.7%, and 3.1%, respectively. As a first attempt to reduce such interferences, H_2 was used as collision gas in the octopole cell at flow rates of either 4 mL/min or 7 mL/min and the effect at *m/z* 28-30 was evaluated in terms of limit of detection (LoD) and background equivalent concentrations (BEC). Only *m/z* 28 became available for analytical measurements in these conditions, similarly to what we obtained in our earlier work where methane was used in a dynamic reaction cell to investigate agglomeration and dissolution of

silica nanoparticles in aqueous suspensions in time resolved mode.[11] Use of the MS/MS mode substantially lowered the LoD and BEC at *m/z* 29 and promising results for the two most abundant isotopes (^{28}Si and ^{29}Si) were obtained by further increasing the gas flow rate to 10 mL/min (Table 3). In an alternative approach, while maintaining Q1 set at *m/z* 28, 29 and 30, respectively, O_2 was added as a reactive gas into the octopole cell to convert the Si^+ ions into SiO^+ ions, which were measured at the corresponding *m/z* ratios of 44, 45 and 46 (Q2). In the MS/MS mass-shift mode, after optimization of the O_2 flow rate (Fig. 2), the signal intensities obtained at *m/z* ratios of 44, 45 and 46 followed the natural isotopic pattern of Si (Fig. 3) and satisfactory results in terms of LoD and BEC where obtained for the three silicon isotopes (Table 3). This indicates that by using O_2 in the MS/MS mode, interference-free determination of silicon *via* all the naturally occurring isotopes becomes feasible, also in complex matrices. A demonstration is given by the analysis of the internal quality control material ISS-BL, a bovine liver sample spiked with soluble silicon, which was prepared in our laboratory for trueness assessment of total silicon determinations in the absence of matrix reference materials based on biological samples having certified concentration values for silicon.[12] As shown in Table 4, using *m/z* 44, 45 and 46 as analytical masses, the found values are in agreement with the target value established by means of three independent techniques.

Optimization of the FFF separation method

The focusing time and starting cross flow values were selected in a way that clear separation of the void peak from the peak originating from the smallest particle size used in this study (20 nm) was ensured, while losses in the void peak were minimized. During the elution step a linearly decreasing cross flow was chosen as a compromise between the need of minimizing adsorption of analyte on the membrane and total time of analysis while achieving a satisfactory peak resolution. This led to the selection of an injection flow of 0.2 mL/min for 3 minutes at an initial cross flow of 0.8 mL/min for the focusing step, whereas in the elution step the starting cross flow of 0.8 mL/min decreased linearly to 0 mL/min during 40 minutes. Further 10 minutes at 0 mL/min were necessary to remove

residual particles from the separation channel, so that total time of an analytical run was 50 min. A transition time of 0.2 min was used and the detector flow rate was set at 0.5 mL/min.

Fig. 4 shows the separation of seven silica particle size fractions from 20 to 180 nm recorded with the ICP-MS/MS detector. All peak maxima are separated, hence allowing attribution of particle diameter in unknown samples in a size-range covering one order of magnitude. In particular, separation of size fractions in the nano-range (≤100 nm) is very satisfactory.

A close examination of Fig. 4 reveals that the peaks corresponding to 120 and 160 nm-silica particles show a tail whereas the other size fractions (including 180 nm-particles) show a relatively narrow and symmetrical peak. The tailing of the two peaks is due to the inherent higher polydispersity of the nanosilica materials with nominal sizes of 120 and 160 nm, as reflected by the size distribution profile in the manufacturer lot certificate showing the presence of few particles sized 170-210 nm and 200-300 nm, respectively. The coefficient of variation of the TEM diameter for the two materials is 12-14% as opposed to an average of 7% for the other materials (range 6-9%) and 10% for the 20 nm-sized particles.

Looking at Fig. 4, it can be noticed that the pure eluent signal recorded as the baseline of the fractogram is relatively high. The FFF eluent was characterized for total silicon content, which resulted in a background of 64.2 ng Si/mL Si contamination of the FL-70 surfactant was the cause and this shows a possible area of improvement of the analytical performance achieved.

Fig. 5 shows the fractograms of a mixture of four silica nanoparticles with nominal sizes of 20, 50, 100, 180 nm recorded with MALS and ICP-MS/MS as the detectors. Concentration dependent effects, e.g. possible channel overloading, resulting in peak asymmetry or shift of retention times with consequent misinterpretation of size results was evaluated. This was achieved by varying the mass load by a factor of 10 to detect any sample concentration related effect over the mass range 0.03-0.26 µg for the investigated quadrimodal mixture. The method was found to be quite robust and no systematic variation in retention time or calculated size could be detected (Table 5).

Recovery was also evaluated by comparing peak-areas obtained for injection of one particle at a time without and with cross-flow, using the mass-calibration approach (post-channel) employed in the whole study. For injections with cross-flow, the area considered was the sum of the void peak and the analyte peak. Recoveries decreased at the highest injected mass only whereas they were generally in the 90-100% range over a wide range of injected mass except for the 100 nm-particle, which uniformly showed a significantly ($p < 0.01$, Kurskal–Wallis test) lower value (50-60%) (Table 5). The reason for the worse recovery of the 100 nm particle is unknown but it appears to be a particle-specific effect not related to the performance of the analytical method in the mass range 0.03-0.26 µg.

Reproducibility of RT was also evaluated on three different days of analysis and turned out to be in the range 2.0-2.4 % for the three smaller particles and 0.2% for the largest one.

Fig. 6 shows the FFF-ICP-MS/MS fractograms for the investigated quadrimodal mixture of silica nanoparticles obtained by recording the signal of each of the three silicon isotopes in the MS/MS mass-shift mode using O_2 as reaction gas. It can be seen that a neat fractogram is obtained even when ^{30}Si, the isotope with the lowest natural abundance, is used, which can be advantageously employed in the analysis of unknown samples to avoid the obtainment of excessively intense silicon signals. More importantly, availability of the three isotopes for analytical purposes gives the possibility to design detection strategies based on the use of isotope dilution.

Analysis of test samples

The FFF-MALS-ICP-MS/MS method developed was applied to the characterization of two test samples, the reference material ERM-FD100 and the silica suspension with 140 nm nominal diameter. Firstly, the recovery of the two particle samples was investigated by both pre-channel mass-calibration with silica nanoparticles and post-channel mass-calibration with elemental standards. The former calibration strategy compensates for the possible loss of sample materials due to interactions between the particles and permeation membrane or other wetted surfaces in the FFF

channel. Other types of material loss (*e.g.* adsorption on tubing walls) can be assessed by comparing pre- and post-channel mass-calibration. No loss of analyte on the membrane surface due to the application of the cross-flow results from the comparison of the total silicon content of the two test samples with the silicon measured with pre-channel mass-calibration. On the other hand, the silicon measured by post-channel mass-calibration is 92% and 72% of the total silicon in the ERM-FD100 and the 140 nm-particle, respectively. Therefore, post channel-calibration with ionic silicon leads to a less accurate quantification, whereas with pre-channel mass-calibration accurate quantification is ensured due to the fact that samples undergo the same injection/separation procedure as the calibrants.

The hydrodynamic diameter of the two test samples calculated either from the radius of gyration (MALS) or by size calibration (FFF-ICP-MS/MS) is compared with the reference values in Table 6. In the latter case, the particle size calibration curve obtained using 7 experimental points (Table 2), with equation $y = 0.1816x^2 - 0.9306x + 11.405$ (y is particle diameter in nm, x is RT in min, $R^2 = 0.993$), was used. The parabolic shape of the size calibration curve is in agreement with other studies that employed FFF as fractionation technique and dealt with nanomaterials having different chemical composition than the present study.[18]

In general, a good agreement between the two experimentally determined values and with the reference value was found. It has to be noted that in FFF-MALS analysis of ERM-FD100 the measured value was close to the size detection limit of the technique[19-20] and a high sample concentration had to be used. In FFF-ICP-MS/MS the smallest particle we measured appeared to be well above the size detection limit of the method, which is probably dictated by the separation capability of asymmetric flow FFF at low particle sizes (around 1 nm)[15].

When size calibration in FFF-ICP-MS/MS is used, hydrodynamic diameters appears to be slightly overestimated. For ERM-FD100, an attempt was made to use a linear calibration curve obtained from the first four size calibration points (≤100 nm) and the resulting value was 19.9±3.3 nm.

Overall, the availability of two measurement approaches in the present method gives greater confidence in the estimation of reliable size values.

Conclusions

Quantitative characterization of silica nanoparticles was accomplished by on-line coupling of asymmetric flow FFF with multiangle light scattering and ICP-MS/MS detection. Accurate dimensional characterization of the particles separated by FFF was achieved by means of both ICP-MS/MS detection with size calibrants and standardless sizing by MALS. Element-specific detection by ICP-MS/MS, pre-channel mass-calibration with silica nanoparticles and post-channel mass-calibration with elemental standards were used to provide quantitative data on the silicon present in the size fractions separated online by FFF. The FFF-MALS-ICP-MS/MS method developed enabled dimensional and mass determination of silica particles over a size range of one order of magnitude with satisfactory recoveries of analyte material.

The capability to use the three silicon isotopes for analytical measurements is an important feature of the method and opens the way to studies involving the use of isotopically enriched silica nanoparticles. The method is currently being used for the detection of nano-sized silica in food items.

Acknowledgments

The authors acknowledge technical support by Paolo Scardina and Peter Planitz (Agilent Technologies), Thorsten Klein and Evelin Moldenhauer (Postnova Analytics), and Roberto Santoliquido (Alfatest).

References

1. European Commission. 2012. Commission staff working paper: types and uses of nanomaterials, including safety aspects accompanying the communication from the Commission to the European Parliament, the Council and the European Economic and Social Committee on the Second regulatory review on nanomaterials. SWD(2012) 288 final, Brussels. Available at http://ec.europa.eu/health/nanotechnology/docs/swd_2012_288_en.pdf, last accessed 14 December 2014.
2. D. Napierska, L.C.J. Thomassen, D. Lison, J.A. Martens, P.H. Hoet, *Particle and Fibre Toxicology* 2010, **7**, 39.
3. T.P.J. Linsinger, G. Roebben, C. Solans, R. Ramsch, *Trends Anal. Chem.*, 2011, **30**, 18–27.
4. T.P.J. Linsinger, Q. Chaudhry, V. Dehalu, P. Delahaut, A. Dudkiewicz, R. Grombe, F. von der Kammer, E.H. Larsen, S. Legros, K. Loeschner, R. Peters, R. Ramsch, G. Roebben, K. Tiede, S. Weigel, *Food Chem.*, 2013, **138**, 1959–1966.
5. L. Calzolai, D. Gilliland, F. Rossi, *Food Addit. Contam.*, 2012, **29**, 1183–1193.
6. P.C.E. van Kesteren, F. Cubadda, H. Bouwmeester, J.C.H. van Eijkeren, S. Dekkers, W.H. de Jong, A.G. Oomen, *Nanotoxicology*, 2014, Epub ahead of print July 18, doi:10.3109/17435390.2014.940408.
7. M. Rossi, F. Cubadda, L. Dini, M.L. Terranova, F. Aureli, A. Sorbo, D. Passeri, *Trends Food Sci. Technol.*, 2014, **40**, 127-148.
8. M.R. Zachariah, D. Chin, H.G. Semerjian, J.L. Katz, *Appl. Optics*., 1989, **28**, 530-536.
9. A. Braun, O. Couteau, K. Franks, V. Kestens, G. Roebben, A. Lamberty, T.P.J. Linsinger, 2011, *Adv. Powder Technol*., **22**, 766–770.
10. R. Peters, E. Kramer, A.G. Oomen, Z.E. Rivera, G. Oegema, P.C. Tromp, R. Fokkink, A. Rietveld, H.J. Marvin, S. Weigel, A.A. Peijnenburg, H. Bouwmeester, *ACS Nano*, 2012, **6**, 2441-2451.
11. F. Aureli, M. D'Amato, B. De Berardis, A. Raggi, A.C. Turco, F. Cubadda, *J. Anal. Atom. Spectrom.* 2012, **27**, 1540-1548.
12. F. Aureli, M. D'Amato, A. Raggi, M. Ciprotti, S. Nisi, A. Sorbo, F. Cubadda, 2014. In preparation.

13. European Commission. Commission Recommendation of 18 October 2011 on the definition of nanomaterial (2011/696/EU). Official Journal of the European Union L 275/38, 20/10/2011.

14. A. Dudkiewicz, K. Tiede, K. Loeschner, L.H. Soegaard Jensen, E. Jensen, R.Wierzbicki, A. Boxall, *Trends Anal. Chem*., 2011, **30**, 28-43.

15. F. von der Kammer, S. Legros, E.H. Larsen, K. Loeschner, T. Hofmann, *Trends Anal. Chem*., 2011. **30**, 425-436.

16. C. Contado, L. Ravani, M. Passarella, *Anal. Chim. Acta*, 2013, **788**, 183-192.

17. J. Heroult, V. Nischwitz, D. Bartczak, H. Goenaga-Infante, *Anal. Bioanal. Chem.*, 2014, **406**, 3919-3927.

18. O. Geiss, C. Cascio, D. Gilliland, F. Franchini, J. Barrero-Moreno, *J. Chromatogr. A*, 2013, **1321**, 100-108.

19. A. Zattoni , D.C. Rambaldi, P. Reschiglian, M. Melucci, S. Krol, A.M. Coto Garcia, A. Sanz-Medel, D. Roessner, C. Johann, *J. Chromatogr. A*, 2009, **1216**, 9106-9112.

20. M. J. Spallek, A. Wallner, R. Jünger, Application Note 0028, Postnova Analytics GmbH.

Tables

Table 1. Optimized instrumental parameters.

Instrument Parameter	Operating Conditions
RF applied power (W)	1550
Carrier gas flow rate (L/min)	0.90
O_2 reaction gas flow rate (mL/min)	1.15
Q1 bias (V)	-1
Octopole bias	-5.3
Acquisition mode	Time Resolved Analysis
Sampling period (sec)	2
Integration time/mass (sec)	0.5
Q1 Selected masses	28, 29, 30, 72
Q2 Selected masses	44, 45, 46, 72

Table 2. Silica nanoparticles suspension used for size calibration.

Nominal size[a] (nm)	TEM diameter[a] (nm)	d_h reference value[a] (nm)	d_h found value[b] (nm)
20	23.2±2.4	24.9	31.2±8.3
50	47.7±3.7	61.6	60.4±10.6
80	82.6±4.7	96.0	103.0±14.7
100	101.7±9.0	116.6	111.2±14.2
120	119.9±16.7	154.7	152.8±16.0
160	156.0±18.1	175.8	167.0±10.8
180	186.8±13.1	221.1	203.1±19.6

[a] Hydrodynamic diameter as reported on the manufacturer's certificate.

[b] Hydrodynamic diameter as assessed by converting r_g values obtained by MALS into d_h according to the relation r_g/r_h= 0.775 ($d_h = 2r_h$) based on the consistent spherical shape of the particles used.

Table 3. Linearity, sensitivity, LoD and BEC of silicon determination by ICP-MS/MS with different cell gases

Analytical conditions	*m/z*	R[a]	Sensitivity[b] *cps*	b (blank)[c] *cps*	LoD[d] *µg/L*	BEC[e] *µg/L*
H_2 10 mL/min MS/MS	$^{28}Si \rightarrow {}^{28}Si$	0.9996	39134	55962	0.09	1.4
	$^{29}Si \rightarrow {}^{29}Si$	0.9984	2195	4501	0.07	2.1
	$^{30}Si \rightarrow {}^{30}Si$	0.0542	986	1875786	69.3	1901.3
O_2 1.15 mL/min MS/MS	$^{28}Si \rightarrow {}^{28}Si^{16}O^+$	0.9998	4876	13472	0.09	2.8
	$^{29}Si \rightarrow {}^{29}Si^{16}O^+$	0.9998	260	782	0.31	3.0
	$^{30}Si \rightarrow {}^{30}Si^{16}O^+$	0.9994	183	1112	0.56	6.1

[a] Correlation coefficient.

[b] Slope of the calibration curve (a) in the equation $y = ax + b$, where y is the measured intensity, x is the analyte concentration and b is the intercept set at zero concentration or blank.

[c] Number of cps in the calibration blank.

[d] Limit of detection calculated as three times the standard deviation of the blank signal counts (b) divided by the sensitivity factor (a), *i.e.* $LoD = \frac{3\sigma b}{a}$.

[e] Background equivalent concentration calculated dividing the analyte concentration (C_s) by the signal-to-background ratio , *i.e.* the net analytical signal (a) divided by the blank signal (b), *i.e.* $BEC = \frac{C_s b}{a}$.

Table 4. Trueness of total silicon determination by ICP-MS/MS (*n*=5).

	Target value[a]	$^{28}Si^{16}O^{+}$	$^{29}Si^{16}O^{+}$	$^{30}Si^{16}O^{+}$
Measured Si concentration (µg/g)	20.4±1.9	20.9±1.8	21.2±2.1	20.0±1.8

[a] Assessed by three independent techniques (ICP-DRC-MS, ICP-OES, HR ICP-MS)[12]

Table 5. Peak retention time (RT), measured size[a] and recovery at varying injected masses for particles with nominal sizes in the range 20-180 nm.

Injected mass *(µg)*	**20 nm**			**50 nm**			**100 nm**			**180 nm**		
	RT (min)	*Size (nm)*	*Rec. (%)*	*RT (min)*	*Size (nm)*	*Rec. (%)*	*RT (min)*	*Size (nm)*	*Rec. (%)*	*RT (min)*	*Size (nm)*	*Rec. (%)*
0.03	12.0	26.5	100	18.7	57.4	92	28.2	129.9	60	37.6	232.9	83
0.05	11.3	24.1	103	18.5	56.2	100	27.8	126.1	48	35.9	211.7	113
0.13	11.5	24.6	102	17.7	52.0	90	26.9	118.1	63	37.0	225.6	106
0.26	11.7	25.3	85	18.7	57.6	73	27.1	119.9	62	36.9	224.3	80

[a] By size calibration

Table 6. Size characterization of two test samples by AF4-MALS-ICP-MS/MS.

Test sample	Reference value (nm)	d_h calculated from r_h as measured by FFF-MALS (nm)	d_h obtained by size calibration in FFF-ICP-MS/MS (nm)
ERM-FD100	19.4±1.3[a]	22.9±4.2	23.3±3.8
NanoXact silica 140 nm	150.4[b]	142.3±10.6	167.4±8.9

[a] Certified value measured by electron microscopy.
[b] Reference value reported on the manufacturer's certificate, measured by DLS.

Figures

Figure 1. Diagram of the analytical platform used. The FFF-MALS-ICP-MS/MS system with pre-channel injection of nanoparticles (A), and post channel injection of ionic calibrant solutions by means of a flow injection system (B) are shown. A switch valve allowed A or B to be operational and a peristaltic pump delivered the internal standard solution.

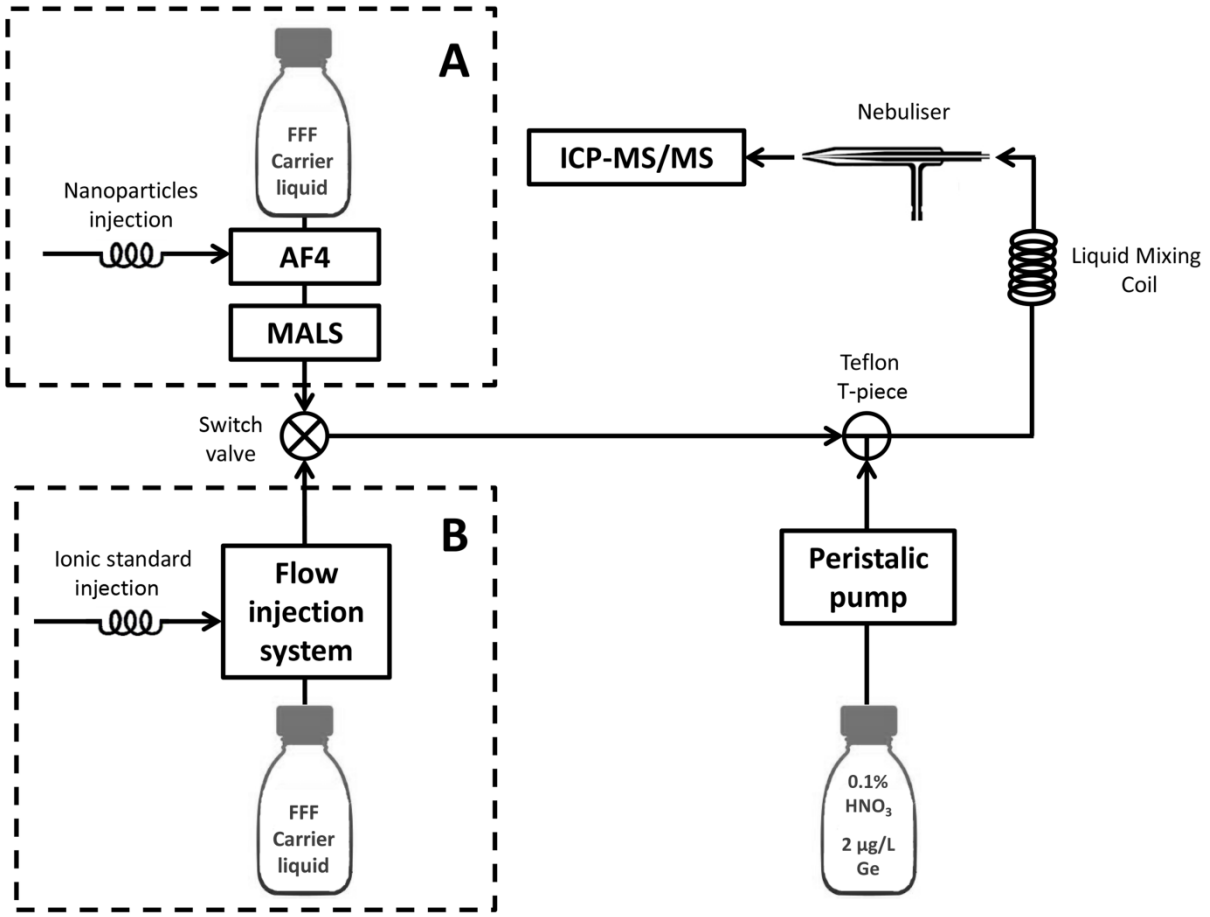

Figure 2. Silicon detection in the MS/MS mass-shift mode: optimization of the O_2 flow rate. Signal intensities are shown as a function of the cell gas flow rate for the FFF carrier liquid (blank, red circles) and a 50 µg/L ionic silicon standard in FFF carrier liquid (green circles). The background equivalent concentration (BEC) is given in blue circles and the corresponding values can be read on the y-right axis.

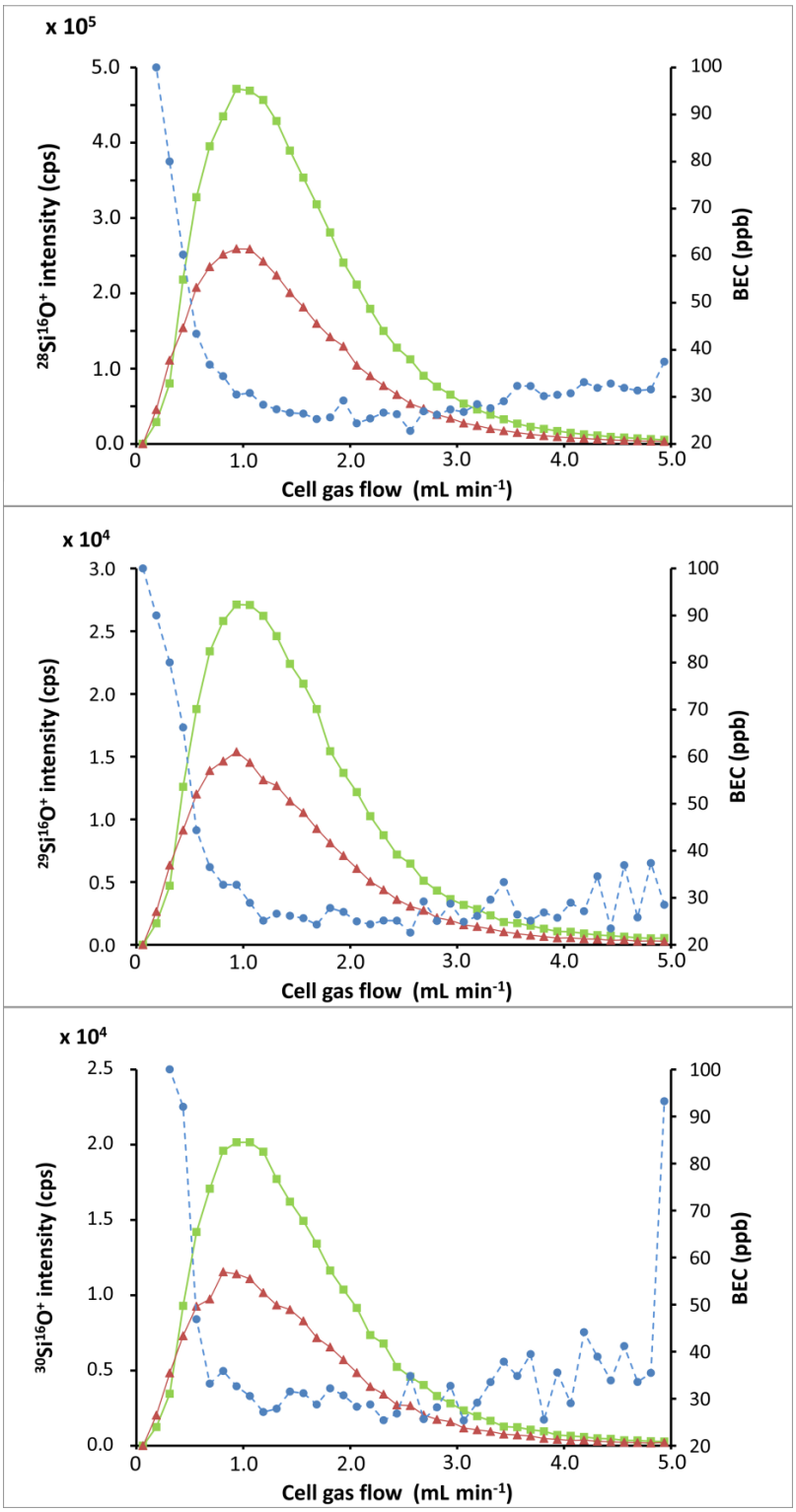

Figure 3. Obtained (blue peaks)[a] and theoretical (red boxes) silicon isotopic pattern.

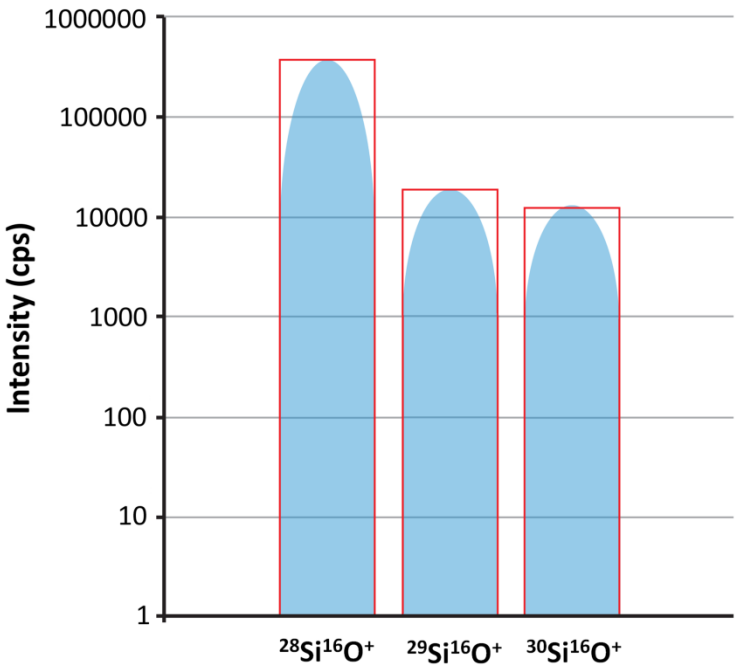

[a] Corrected to account for the oxygen isotopic composition and the contribution of $^{28}Si^{17}O^{+}$ at *m/z* 45 and of $^{28}Si^{18}O^{+}$ at *m/z* 46.

Figure 4. Overlaid FFF-ICP-MS/MS fractograms of silica particle mixtures. Numbers above the peaks represent the nominal size of each fraction in nm.

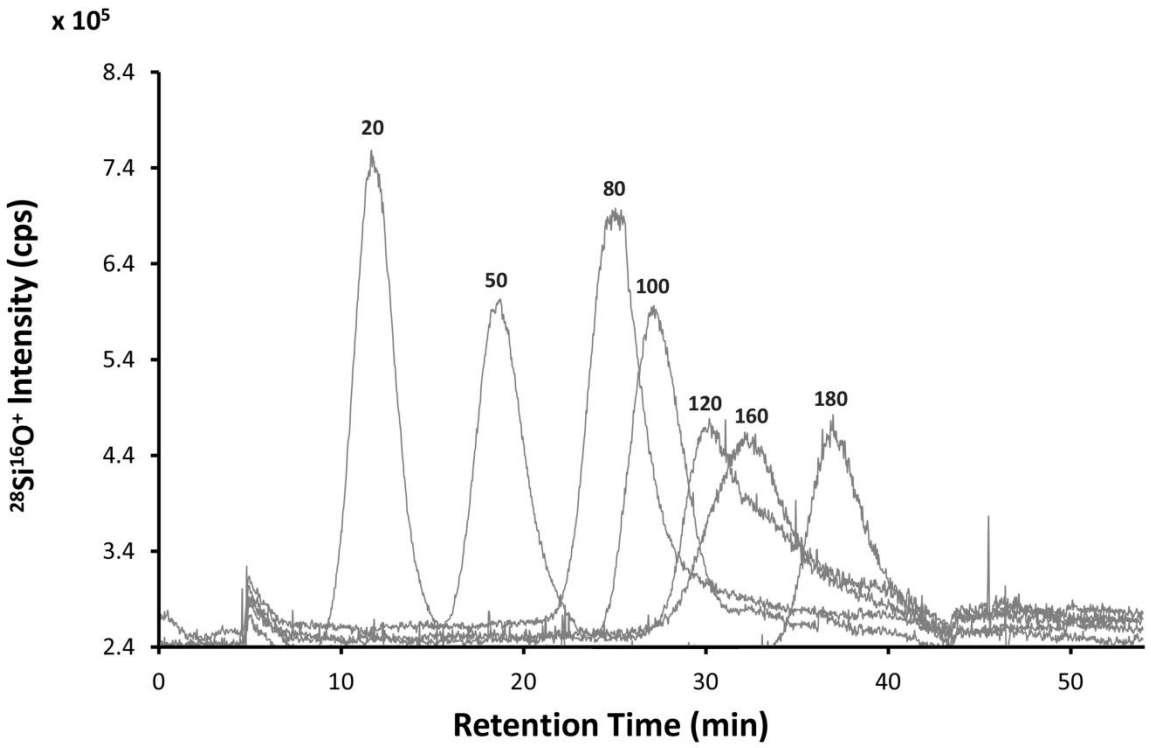

Figure 5. Fractograms of a mixture of four silica nanoparticles with nominal sizes of 20, 50, 100, 180 nm recorded with MALS (lower) and ICP-MS/MS (upper) detectors. Primary left y- axis includes the response for the 92° (MALS) and the $^{28}Si^{16}O^{+}$ signal (ICP-MS/MS), respectively. Radii of gyration are shown in red color across each peak of the lower plot (see the y-right axis for the corresponding values).

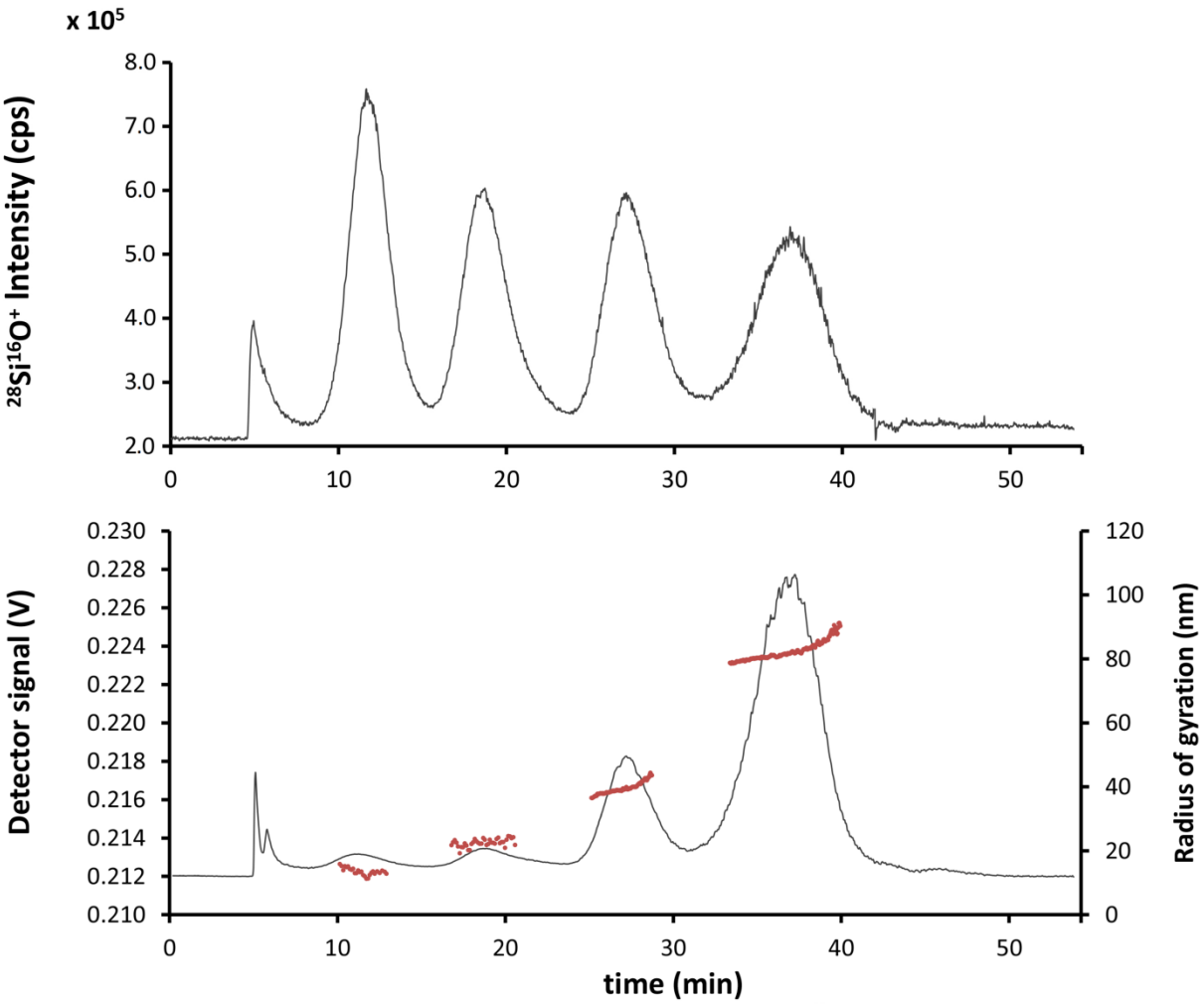

Figure 6. FFF-ICP-MS/MS fractograms of a quadrimodal mixture of silica nanoparticles obtained by recording the signal of $^{28}Si^{16}O^{+}$ (red, left axis), $^{29}Si^{16}O^{+}$ (green, right axis), and $^{30}Si^{16}O^{+}$ (blue purple, right axis).